PERGAMON

Acta mater. 48 (2000) 239–251

Acta MATERIALIA

www.elsevier.com/locate/actamat

LAYERED MAGNETIC STRUCTURES IN RESEARCH AND APPLICATION*

P. GRÜNBERG

Forschungszentrum Jülich-IFF, 52425 Jülich, Germany

(*Received 1 June 1999; accepted 15 July 1999*)

Abstract—An overview is given on the status of research and applications in the field of layered magnetic structures and the historical development is indicated. Currently the research on interlayer exchange coupling, giant magnetoresistance and tunnel magnetoresistance is particularly active, therefore the basic understanding of these phenomena, the size of the effects, important issues and applications are discussed in some more detail.

Keywords: Layered magnetic structures and superlattices; Magnetoresistive effects; Ferromagnetic hysteresis; Interlayer exchange coupling

1. HISTORICAL INTRODUCTION

After Faraday in 1845 had discovered the rotation of the polarization of light in a specimen of glass which was subjected to a magnetic field [1], this effect—which was named after him—became the main driving force for research in thin magnetic films. Faraday himself—albeit unsuccessfully—had tried to see the rotation in thin films of diamagnetic Au but it was not until 1884 that Kundt [2] showed that it could indeed been seen in thin ferromagnetic films. A hundred years later, around 1950, the proportionality between Faraday rotation and magnetization was well established [3] and the improvements in the preparation techniques for thin metallic films enabled experiments on a much larger basis. During the 1950s there was a tremendous increase in the activities which was summarized in a review article by Bean [4].

After a theoretical prediction, made by Neel in 1954 [5] that special anisotropies should appear at surfaces and interfaces, the experimental proof for such an anisotropy was made taking as sample a thin film of Ni [6]. In recent years it has been demonstrated that in this way in fine layered structures strong anisotropies can be obtained and even the influence of interface roughness could be clearly identified [7]. Special anisotropies can also occur due to the presence of an antiferromagnetic material adjacent to the ferromagnetic film [4] when the magnetization M_s at the surface of the antiferromagnet is not completely compensated. Then the hysteresis curve of the ferromagnet can be shifted due to M_s. This phenomenon is also called "exchange anisotropy".

Due to the improvements in evaporation techniques in 1986 the time was right for another discovery, namely the interlayer exchange interaction which was found in three different laboratories for three different structures practically at the same time [8–10].

Other discoveries were made in the area of transport phenomena. In 1857 Thomson, who later became Lord Kelvin, had discovered the anisotropic magnetoresistance (AMR) effect which is a bulk effect [11]. The first magnetoresistance effect which from its nature is not a bulk effect but requires as essential elements interfaces was the tunnel magnetoresistance effect (TMR), discovered in 1975 [12]. In 1988 another thin film magnetoresistance effect—also known as giant magnetoresistance effect (GMR)—was discovered [13–15]. Research on GMR also led to a revival of the interest in TMR and as a result considerable improvements were made concerning the size of TMR [16, 17]. In the following sections we will describe some of the most important aspects of research on interlayer exchange coupling, GMR and TMR.

Let us now turn to the applications. In the 1950s and 1960s ferrite core memories were used as magnetic random access memories (MRAMs) in computers. There was an attempt to replace them by memories consisting of small permalloy patches and

* The Millennium Special Issue — A Selection of Major Topics in Materials Science and Engineering: Current status and future directions, edited by S. Suresh.

1359-6454/00/$20.00
PII: S1359-6454(99)00297-9

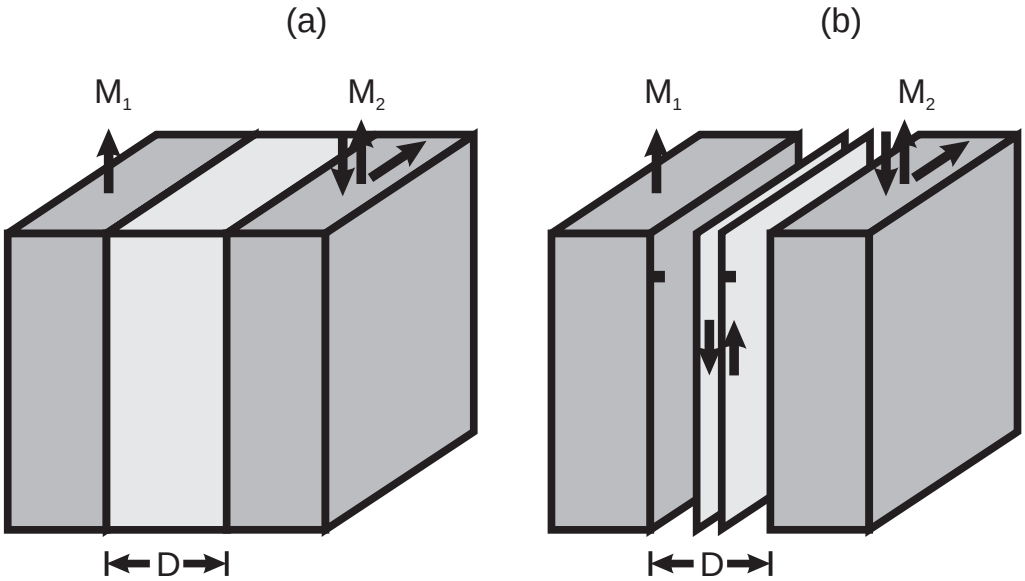

Fig. 1. Illustration of two types of interlayer coupling, depending on the nature of the interlayer. Ferromagnetic films are indicated by dark greytone and interlayers by light greytone. (a) Interlayer is assumed to display no static magnetic order. (b) Static order in the interlayer is assumed, here with antiferromagnetic alignment of successive monolayers. The magnetization M_1 in both (a) and (b) is assumed to point upwards. Due to the coupling the magnetization M_2 can show the basic alignments parallel, antiparallel or perpendicular with respect to M_1.

to use the AMR effect for read out. This failed, and the MRAMs instead were replaced by dynamic random access memories (DRAMs) consisting essentially of capacitors. On the other hand thin magnetic films replaced more and more particulate media for data storage on disks, a trend which currently includes tapes too. For example for hard disks, CoCrPtTa alloy films with coercivities around 3 kOe are now in use. Thin magnetic films became more and more attractive not only for storage media. In 1979 IBM introduced thin film heads for read out from hard disks. Both the write and the read processes were still inductive but the coil was made using thin film technology. In 1992 AMR was introduced for read out which resulted in an annual growth rate of storage capacity of around 60%. Currently AMR is replaced by GMR. And finally there is also a revival of the old MRAM idea where the TMR effect should serve for read out.

2. INTERLAYER EXCHANGE COUPLING

2.1. Phenomenological description, definition of parameters

We restrict ourselves here to the coupling of films made from magnetic 3d elements and/or their alloys, across metallic interlayers. Three basic types of coupling have so far been identified: ferromagnetic (F)-type, antiferromagnetic (AF)-type and 90°-type. Provided there is no anisotropy, then any of these couplings in pure form produces the corresponding alignment of adjacent magnetizations M_1 and M_2. However, both F- or AF-type coupling can be superimposed with 90°-type with the result that the enclosed angle has some odd value. Mostly in addition there is anisotropy that can stabilize a particular alignment.

For a phenomenological description we have to distinguish between the case were the interlayer consists of a material with no static magnetic order and one where such an order is present. In Fig. 1 the two cases are indicated. In part (a) there is no static order and the coupling is thought to be mediated by the conduction electrons of the interlayer. In part (b) antiferromagnetic order in the interlayer is assumed, based on direct exchange. In the figure all moments in an atomic plane parallel to the interface are assumed to be parallel, with the direction alternating between up and down from one plane to the next. Conceptually other types of static magnetic order could also be considered [18], including ferromagnetic interlayers.

As an experimental example for the case displayed in Fig. 1(a) we could think of any paramagnetic or diamagnetic interlayer material like, for example, Au (see below). Experimental examples for the case displayed in Fig. 1(b) are structures with Cr or Mn interlayers. Since both Cr and Mn are metals there can be in addition some interaction of the type displayed in Fig. 1(a).

We consider a structure consisting of only two magnetic films, interspaced by a diamagnetic or paramagnetic interlayer. The following expression for the interlayer coupling areal energy density E_i

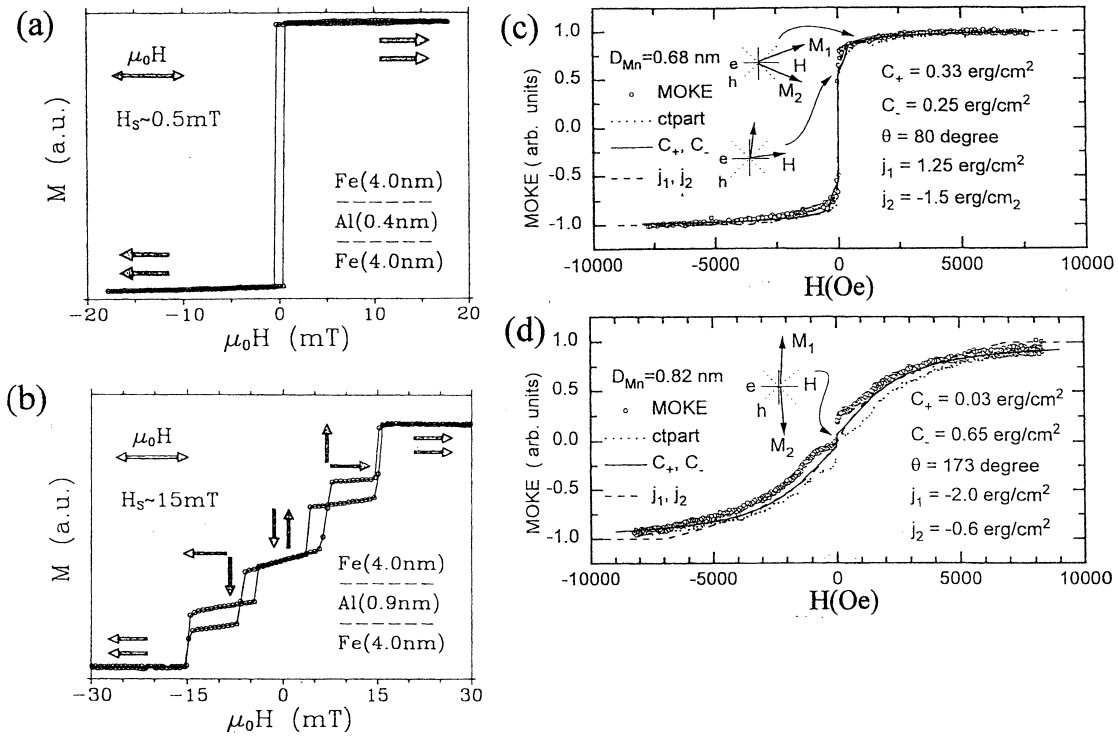

Fig. 2. Remagnetization curves from (a), (b) Fe/Al/Fe layered structures and from (c), (d) Fe/Mn/Fe structures, measured by means of the magneto-optic Kerr effect. The curves in (c) and (d) have been evaluated both on the basis of equations (1) and (2). The corresponding parameters J_1, J_2, C_1, C_2 are indicated.

describes the three "basic" alignments F, AF, 90°, by means of minima of E_i:

$$E_i = -J_1 \frac{\vec{M}_1 \cdot \vec{M}_2}{|\vec{M}_1| \cdot |\vec{M}_2|} - J_2 \left(\frac{\vec{M}_1 \cdot \vec{M}_2}{|\vec{M}_1| \cdot |\vec{M}_2|} \right)^2$$
$$= -J_1 \cos(\Delta\varphi) - J_2(\cos(\Delta\varphi))^2. \quad (1)$$

Here $\Delta\varphi$ is the angle between the magnetizations $\vec{M}_1$ and $\vec{M}_2$ of the films on both sides of the interlayer. The parameters J_1 and J_2 describe the type and the strength of the coupling. If the term with J_1 dominates then from the minima of equation (1) the coupling is F (AF) for positive (negative) J_1, respectively. In the same way if the term with J_2 dominates and is negative we obtain 90°-coupling. The first term on the left-hand side of equation (1) is often called bilinear and the second biquadratic coupling.

At this stage equation (1) is purely empirical. Heuristically, the RKKY interaction, which can be written in the form of a scalar product of the spins (see, e.g. Ref. [18]), together with the fact that in the transition metals we mainly have spin magnetism, can be taken as justification for the first term on the right-hand side of equation (1). Experimentally it has been verified by means of magnetic resonance experiments [19].

Studies of the interlayer coupling however have also included cases of ordered magnetism in the interlayer—so far only antiferromagnetic. It is not important whether the antiferromagnetic order is only due to the interactions in the interlayer or to the interaction with the ferromagnetic films. Tacitly it is often assumed that the latter is the case, hence the interlayer is said to display "proximity magnetism" [18]. This has been shown to exist in the case of Cr [20–24] and Mn [25], adjacent to Fe.

Let us consider for simplicity an antiferromagnet consisting of ferromagnetic monolayer sheets stacked upon each other in the direction of the sample normal, each sheet being magnetically aligned antiparallel to the previous one. Such a situation is indicated in Fig. 1(b). This type of interlayer coupling is not due to an indirect exchange mediated via the conduction electrons of the interlayer but is given by the direct exchange of the neighbouring monolayer sheets inside the antiferromagnet and at the interface with the ferromagnet. It is therefore not surprising that the expected functional form of the interlayer coupling energy E_i is now different from equation (1). Slonczewski [18] showed that in this case equation (1) should be

replaced by

$$E_i = C_+\{\Delta\varphi\}^2 + C_-\{\Delta\varphi - \pi\}^2 \qquad (2)$$

where $\Delta\varphi$ as before is the angle between the magnetizations on both sides of the interlayer, but its sign has to be chosen in such a way that $|\{\Delta\varphi - \pi\}| \leq \pi$. C_+, C_- are adjustable parameters. Equation (2) reflects the fact that E_i should have a minimum for $\Delta\varphi = 0$ in the ideal case of an odd number of monolayer sheets (ferromagnetic coupling, $C_- = 0$) and $\Delta\varphi = \pi$ the same for even (antiferromagnetic coupling, $C_+ = 0$). The origin of the square dependence in equation (2), as opposed to the cos-dependence in equation (1), lies in the fact that in Fig. 1(b) the source of the coupling energy lies in the interaction between nearest neighbour sheets whose moments are twisted only slightly away from perfect alignment. Then in a series expansion of the coupling energy we need only to consider the square term (the linear part disappears due to the fact that positive and negative twist away from perfect alignment should yield the same energy). This dependence on the square of the twist angle between nearest neighbour sheets translates into a dependence of the total energy on $\{\Delta\varphi\}^2$ for an odd and on $\{\Delta\varphi - \pi\}^2$ for an even number of monolayers, as seen in equation (2).

In general both C_+ and C_- are finite. This can for example happen if the interlayer consists of patches with an even surrounded by such with an odd number of monolayers. Ferromagnetic coupling (C_+) could also be introduced by the presence of pinholes and magnetic bridges, hence equation (2) is also suited for a description of this case.

The 90° coupling is obtained when C_+ and C_- in equation (2) are of equal size. This 90° coupling differs from the one due to the second term in equation (1). If equation (1) is valid there is saturation at a well-defined finite field value, whereas in the case of equation (2) there is only asymptotic saturation. Experimentally this is the most important criterion to distinguish between the two cases.

2.2. *Representative experimental examples*

Interlayer coupling can be measured from a detailed analysis of remagnetization curves and from the frequencies of coupled spinwaves [26, 27]. As an example we display in Fig. 2 remagnetization curves from Fe/Al/Fe layers [panels (a) and (b)] and Fe/Mn/Fe layers [panels (c) and (d)] [28]. In Fig. 2(a) the coupling is ferromagnetic hence the films reverse their magnetizations always in unison. In this case the coupling strength cannot be determined. In Fig. 2(b) antiferromagnetic- and 90°-type coupling are superimposed, which for proper field values produce the corresponding alignments as shown. Since Al is paramagnetic equation (1) should be used for the evaluation. In Figs 2(c) and (d) interlayers of Mn with different thickness have been employed. The curves have been evaluated using equation (2), yielding the C_+ and C_- parameters as shown. Note that in Fig. 2(c) C_+ and C_- are of similar size therefore we expect mainly 90°-type coupling whereas in Fig. 2(d) C_- dominates, therefore the coupling should be mainly antiferromagnetic. For Figs 2(c) and (d) an evaluation based on equation (1) with parameters J_1 and J_2 has also been performed and is shown for comparison. Note that the J_1–J_2 fit and the C_+–C_- fit agree rather well in the small field range but for larger field values the J_1–J_2 fit is not quite as good as the C_+–C_- fit. Hence the approach to saturation is better described by equation (2).

In Fig. 3 we see the result of such evaluations as a function of interlayer thickness for a Fe/Au/Fe structure in part (a) and for Fe/Mn/Fe in part (b). Equation (1) has been used for (a) and equation (2) for (b). Positive values in (a) have been obtained using the "spin engineering" technique [29]. In this case additional layers including those with antiferromagnetic coupling are added to the structure of which ferromagnetic coupling has to be determined and then its strength can also be measured.

In Fig. 3(a) for small d_{Au} the coupling is strongly ferromagnetic, probably due to pinholes and magnetic bridges. For increasing d_{Au} ferromagnetic coupling quickly decreases, until there are oscillations around zero. The negative values representing antiferromagnetic- or 90°-type coupling are also seen in the inset on an enhanced scale. One can clearly see oscillatory behaviour with attenuation as a function of the interlayer thickness. Two oscillation periods are superimposed. In a recent study of the Fe/Au/Fe system using an Fe whisker as substrate [30] the two periods have been verified but due to the excellent growth conditions in that case the coupling was much stronger. Multiperiodic, attenuated behaviour has been seen in many cases and is characteristic of interlayer exchange coupling. The interaction leading to the coupling across an interlayer with static magnetic order, as in Fig. 1(b), is the standard nearest neighbour direct exchange, applied to a chain of spins. The interaction mediated by the metal electrons as in Fig. 1(a) is somewhat more complicated. We will sketch qualitatively some details of its origin in the next section.

2.3. *A physical picture for the origin of the coupling mediated by metal electrons*

The basic assumption within the quantum well approach, in order to explain oscillatory coupling, is spin-dependent reflectivity of electrons at the non-magnetic/magnetic interfaces [31–33]. In Fig. 4(a) strong reflectivity at the interfaces is assumed for those electrons which have their spins opposite

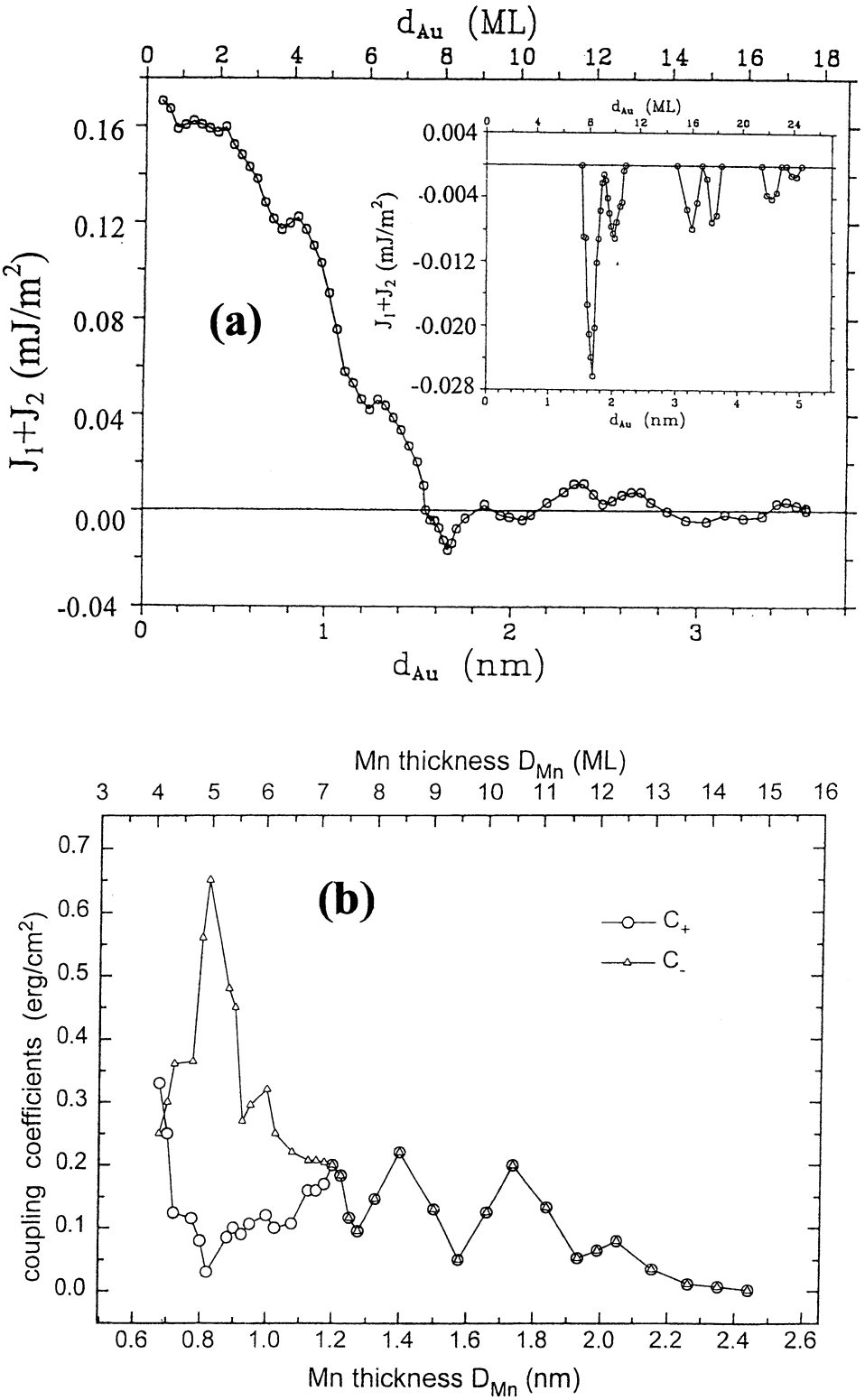

Fig. 3. Strength of interlayer exchange coupling in (a) Fe/Au/Fe and in (b) Fe/Mn/Fe. Negative values in (a) correspond to antiferromagnetic- or 90°-type coupling. An enhanced view of the latter is shown in the inset.

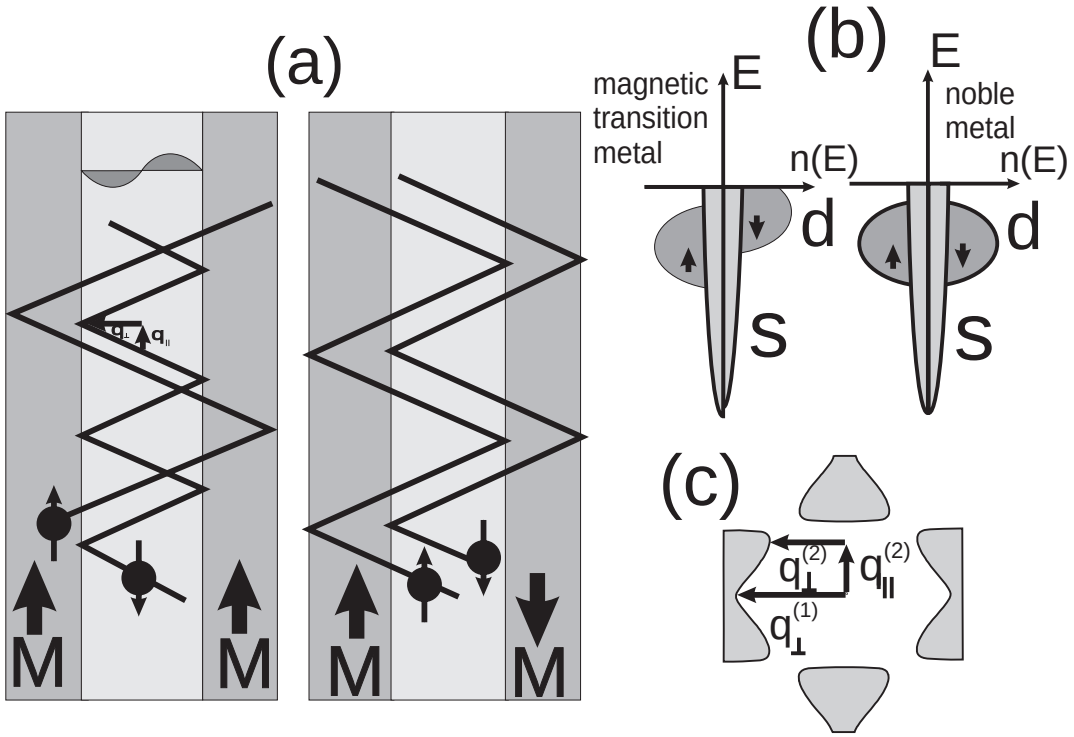

Fig. 4. (a) A layered magnetic structure with parallel and antiparallel magnetization alignment and the propagation of electron waves with spin up and down. For parallel alignment the wave with spin down is confined and forms a standing wave. (b) The reason for the various reflectivities, taking schematic band structures for magnetic 3d metals and noble metals as interlayers as examples. (c) Two stationary vectors, $q_\perp^{(1)}$ and $q_\perp^{(2)}$, in the [100] direction are shown, taking the Au Fermi surface as an example.

to the local magnetization, and weak reflectivity for the others. The reason for such a behaviour is indicated in Fig. 4(b), using schematic band structures for the magnetic 3d transition metals and noble metals as examples. For reasons that will become clearer below, we can restrict ourselves to electrons at the Fermi level. Then, for the chosen example, for spin up electrons we have s-states at the Fermi energy for both the 3d transition metals and the noble metals, as is indicated by the similar densities of states in Fig. 4(b). This leads to a good transmission. For spin down electrons on the other hand, due to the splitting of the energies in the magnetic films we have mixed d- and s-states at the Fermi level for the transition metal, hence the transmission of the electrons from the noble metal is reduced. Based on the spin-dependent reflectivity there is a strong (weak) confinement in the interlayer for spin down (up) for parallel magnetization alignment as on the left-hand side of Fig. 4(a) whereas for the antiparallel alignment the reflectivities are as shown on the right-hand side and the confinement is lost.

Hence parallel magnetization alignment is characterized by a confinement of part of the electrons and there are characteristic energy changes associated with this, which makes this situation for certain interlayer thickness more and for others less favourable than antiparallel alignment for which case the confinement is lost. Due to the confinement the motion of the electrons perpendicular to the interfaces becomes quantized and we obtain a spectrum of discrete energy levels corresponding to the formation of standing electron waves. Such a standing wave is indicated in Fig. 4(a) and is the result of the superposition of two propagating waves with wavevector components $\pm q_\perp$. For a standing wave to form we must have $|2q_\perp| = n \cdot 2\pi/D$ (n is an integer and D is the interlayer thickness). When the interlayer thickness is increased the discrete levels shift downwards and are populated upon crossing the Fermi energy E_F. Hence it is plausible that there are oscillations of the electronic energy due to the fact that discrete energy levels become populated. It turns out that these oscillations favour parallel alignment for certain thicknesses and antiparallel alignment for others. Hence the interlayer coupling oscillates as a function of the interlayer thickness D due to oscillations in the electronic energy. The oscillation period λ_D is given by the difference in D where two subsequent discrete energy levels cross the Fermi energy, hence $\lambda_D = 2\pi/|2q_\perp|$, where $q_\perp$ is taken from the Fermi surface.

Hence oscillatory coupling can be traced back to changes in the densities of states which come as a

result of confinement. The stronger the confinement and the higher the changes in the density of states the larger will be the associated amplitudes. At this point it is important to consider that not all possible wavevectors $q_\perp$ from the Fermi surface contribute in the same way. Some are associated with higher densities of states than others and therefore contribute more in the above consideration.

Let us discuss this situation for our example of noble metal interlayers and choose the [100] orientation for the normal to the interface. Figure 4(c) reveals that along [100] two wavevectors $q_\perp^{(1)}$ and $q_\perp^{(2)}$, as indicated, are associated with particularly high densities of states, because their lengths change only very little upon a slight shift up or down. They are called stationary vectors and generate two superimposed oscillations of the coupling as a function of the interlayer thickness. Here $q_\parallel^{(2)}$ and $q_\perp^{(2)}$ correspond approximately to the situation shown in Fig. 4(a) and $q_\parallel^{(1)} = 0$.

From Fig. 4(a) it is clear that $q_\perp$ of Fig. 4(c) should be chosen along the crystallographic direction, determined by the surface normal of the sample. Hence we expect a dependence of the oscillation periods on the chosen growth direction, which has indeed been verified [34, 35].

From the foregoing discussion it seems that only the value of $q_\perp$ is relevant for the interlayer coupling, $q_\parallel$ having no significance. Due to the translational symmetry in the plane of the film, however, $q_\parallel$ must be conserved upon reflection and transmission of the electron wave (in optics this leads to specularity and the law of refraction). In the present case, if the reflection is not complete then $q_\parallel$ must be conserved for the wave which penetrates the magnetic layer. Due to multiple interference effects in the magnetic layer the reflectivity can depend on its thickness. This eventually leads to a magnetic thickness dependence of the interlayer coupling [36, 37]. In a similar way a "cap" layer dependence can also be considered and has been observed [38, 39].

2.4. Interlayer materials dependence

From the foregoing considerations follows that in order to get a strong coupling a large contrast in the spin-dependent reflectivity is expected to be favourable. As was pointed out experimentally [40] and theoretically [41] such a good spin contrast can occur when the material of the magnetic films and the interlayer are taken from the same, or close, columns of the periodic table. Indeed a record value of $34\,\mathrm{mJ/m^2}$ for antiferromagnetic coupling has been found for the coupling of Co across Rh [42].

Further dependence of the coupling on the position of the interlayer material in the periodic table and the question whether the case displayed in Fig. 1(a) or (b) is more appropriate has to include also the tendency of the interlayer to ferro- or antiferromagnetism. For Cr and Mn interlayers the proximity effect, leading to antiferromagnetic order even much above the bulk Neel point, is well established [20–25]. (For Cr the situation is even more complicated because of the spin-density wave-type antiferromagnetism [20–24].) Palladium is expected to show a tendency towards ferromagnetism. It is in agreement with the fact that for Pd interlayers the coupling was mostly found to be ferromagnetic [43–45] with at most weak antiferromagnetic coupling.

Obviously for metallic interlayers, displaying static magnetic order, in addition to the direct interaction described by equation (2) there can also be the indirect type described by equation (1). Possibly the short periods (2 ML) in the case of Cr and Mn are due to the direct interaction whereas long periods which are also observed are due to the indirect mechanism. It turns out that the observed coupling strengths are of similar size. This is surprising because one would expect that the direct exchange—even though being active "only" via a chain—would produce a much stronger coupling. Indeed Vohl *et al.* [46] showed that the direct exchange in ferromagnetic materials expressed in terms of "interlayer coupling" between nearest neighbour atomic planes (e.g. $180\,\mathrm{mJ/m^2}$ acting across 0.14 nm for Fe) is about two orders of magnitude larger than typical values for interlayer exchange coupling ($1\,\mathrm{mJ/m^2}$). In a chain this value would decrease linearly as a function of the chain length. Furthermore, Mirbt *et al.* [47] calculated the difference in coupling for paramagnetic and antiferromagnetic Cr and found an increase of more than an order of magnitude in the ordered case. On the other hand it is well known from the phenomenon of "exchange anisotropy" (see Section 1) that at a ferromagnetic/antiferromagnetic interface there can be strong frustration effects and hence weakening of the effective coupling, due to interface roughness. Proximity effects as well as the influence of roughness have recently been discussed in detail in an excellent review by Pierce and co-workers [20–24].

Studies of the coupling have also included interlayers of semiconductors and insulators [48, 49]. In particular Si interlayers were studied in detail. Strong antiferromagnetic coupling has indeed been observed for Fe across Si but it is now believed to be mainly due to the formation of half-metallic Fe silicide [50, 51].

So far we have dealt with ferro- and antiferromagnetic coupling and oscillations between the two. The 90° coupling could also be explained as an intrinsic effect, which occurs in a higher order of perturbation theory. The most likely mechanism however seems to be the "fluctuation mechanism" due to interface roughness, proposed by Slonczewski [18].

3. GIANT MAGNETORESISTANCE (GMR)

3.1. First observations

Figure 5 shows the first observations in multilayers (A) and double layers (B) [13–15]. Currents are in-plane. Due to antiferromagnetic interlayer coupling the magnetization alignment of the neighbouring Fe films in small fields is antiparallel and the resistance is high. Increasing the field aligns the magnetizations parallel and the resistance drops. In multilayers (A) the effect is much stronger than in double layers (B) which is an indication that the number of available interfaces plays an important role. The term giant magnetoresistance (GMR) referred originally to the large size of the effect in multilayers but is now generally used for magnetoresistance due to non-parallel magnetization alignment. The largest effect occurs when an AF alignment by an applied field is changed into a F alignment. The AF alignment can be provided by AF interlayer exchange as in Fig. 5 or by other means (see below). Then oscillatory coupling also gives rise to oscillations of the GMR effect.

An antiparallel arrangement can also be obtained by other means, for example by different coercivities of successive magnetic layers [52, 53], or by pinning the magnetization using an antiferromagnetic material in direct contact, known as "exchange biasing". If GMR is obtained via one of these methods and not via AF interlayer coupling, usually the term "spin valve system" is used in the literature although there is no difference concerning the mechanism of the GMR effect. Such a case is displayed in Fig. 6 [52]. The sample is a Co/Au/Co layered structure with one of the Co films deposited directly onto the GaAs substrate. Since this Co film is more strained than the one prepared on the Au interlayer, it has a higher coercivity. During magnetization reversal of the whole structure it reverses later than the other, resulting in a small field range where the alignment is antiparallel. In Fig. 6(A) this range is marked by antiparallel arrows. The curve in Fig. 6(B) shows the associated electrical resistance $R(H)$ and its increase due to the antiparallel alignment.

The GMR effect has been investigated in two different geometries, namely the "CIP" (current in-plane) [13–15] and the "CPP" (current perpendicular plane) geometry [54, 55]. The relative effect is stronger in the CPP geometry, but due to the extremely unfavourable situation (lateral dimensions some orders of magnitude larger than film thickness) the voltage drop perpendicular to the layers, in the CPP geometry, is very difficult to detect.

3.2. Microscopic origin

In order to understand the mechanism leading GMR it is important to remember that only the electrons with energies close to the Fermi edge contribute to the transport. They propagate with high speed but arbitrary direction through the layered structure. In Fig. 7 paths between two reflections at outer surfaces are shown, with scattering events in between. In order not to confuse the picture the changes in direction due to the scattering events are suppressed. An applied voltage gives rise to an acceleration of the electrons in the direction of the electric field, for example in the layer plane (CIP) or perpendicular to it (CPP). The scattering processes are the cause of electric resistivity.

In Section 2.3 it was seen that interlayer coupling can be explained on the basis of a spin-dependent interface reflectivity. Similarly GMR can be explained as due to spin-dependent scattering [13]. Let us assume that electrons with their spins parallel (antiparallel) to the local magnetization are scattered weakly (strongly). The reason could be that for the spin down electrons at E_F according to Fig. 4(b) there are more final states after the scattering

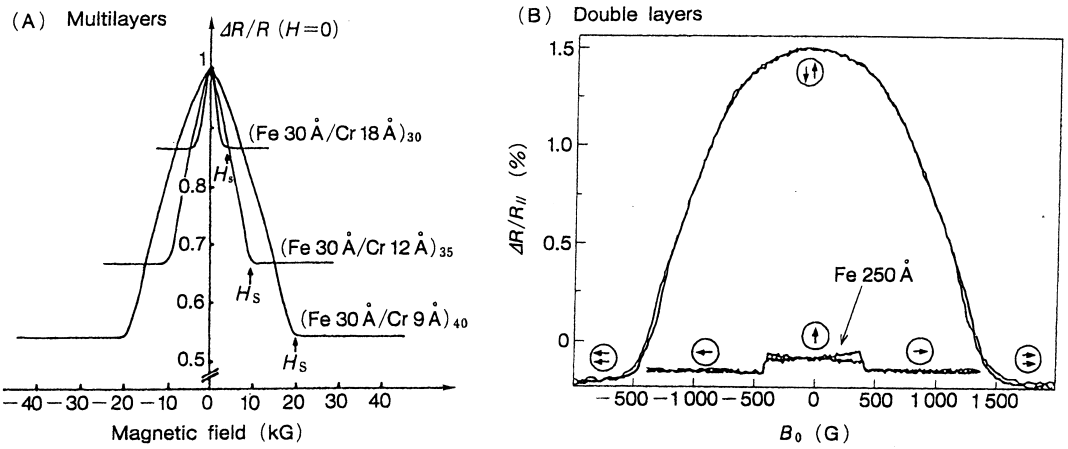

Fig. 5. GMR effect in a multilayer (A) and a double layer (B) of Fe interspaced by Cr. (B) The AMR effect in a single film of Fe with thickness 250 Å is also shown for comparison.

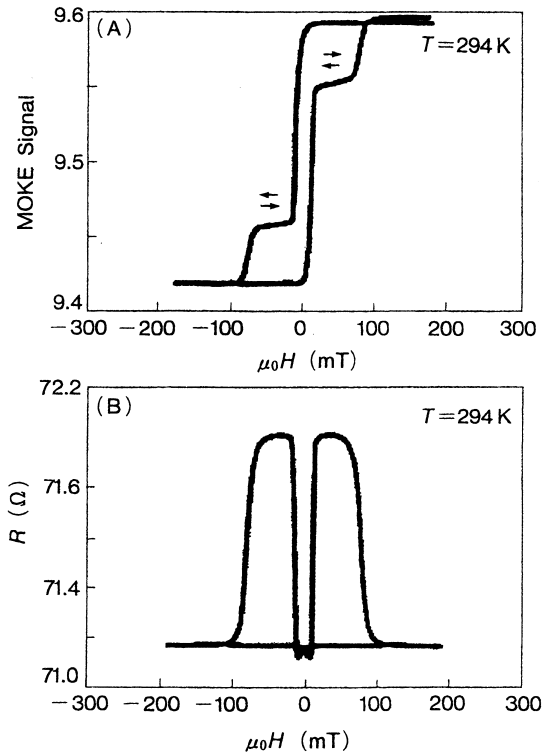

Fig. 6. Remagnetization curve (A) and GMR effect (B) in a Co(100 Å)/Au(60 Å)/Co(100) structure with a hard and a soft Co film.

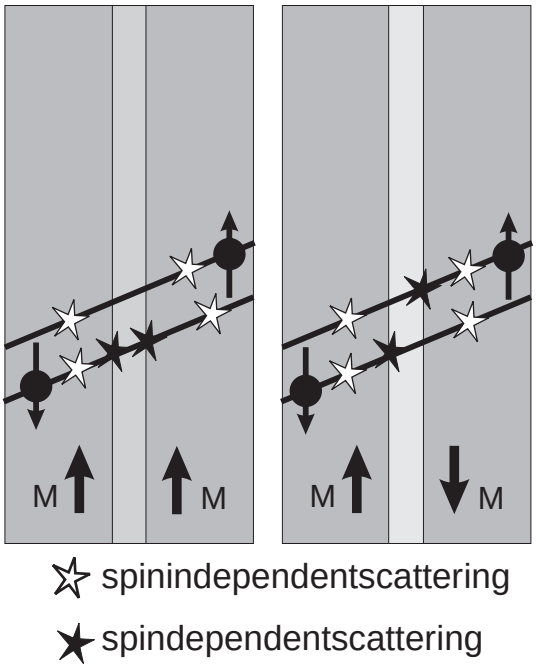

Fig. 7. Electron scattering in magnetic double layers with parallel (left) and antiparallel (right) magnetization alignment. Spin-independent scattering is assumed in the bulk and spin-dependent scattering at the interfaces.

available, than for those with spin up. If we assume that in Fig. 4 those electrons which are reflected more strongly also display larger scattering at irregularities we arrive at the same result. There is a similar situation in optics where a large change in refractive index at an interface leads both to larger reflectivity and larger scattering in the presence of irregularities such as roughness.

In order to demonstrate spin-dependent scattering leading to the GMR effect, we use the simple consideration displayed in Fig. 7. Here we neglected scattering inside the interlayer and there are equal rates of spin-dependent and spin-independent scattering in the ferromagnetic films. The spin-dependent scattering has been assumed to take place at the interfaces where only electrons with spin antiparallel to the local magnetization are assumed to be scattered. According to the "two-current model" invented by Mott [56] the total current can be divided into two currents in parallel—one with spin up (I_+) and one with spin down (I_-). If we assume that one scattering event contributes to the total resistance by an amount r then on the left-hand side I_+ is associated with resistance $2r$ and I_- with resistance $4r$. Hence for parallel alignment the total current $I = I_+ + I_-$ has resistance $R_p = 2r \times 4r/(2r + 4r) = 8r/6$. In the same way we obtain for antiparallel alignment for the total current resistance $R_{ap} = 3r \times 3r/(3r + 3r) = 9r/6$. Hence there is an increase of the resistance due to antiparallel magnetization alignment and the GMR $= (R_{ap} - R_p)/R_p$ in the present case would have a value of 12.5%.

For double layer systems the strongest measured GMR effects are around 17% [57] hence a distribution of the rates as in Fig. 7 seems realistic. Note however that for this consideration a distinction between bulk and interface scattering is not relevant for the strength of the effect, only the spin dependence is important. Indeed there has been a long discussion about whether GMR is more a bulk or an interface effect. We will come back to this question in the next section.

It has been indicated that spin-dependent *scattering* is not the only possibility to explain the GMR effect. For proper materials spin-dependent *reflectivity* could also provide a possible explanation [58]. In this case confinement and the occurrence of quantum well states would also have to be considered [59]. From the observation of interlayer coupling and its explanation given in Section 2.3 it is in fact clear that these phenomena exist.

3.3. Bulk vs interface scattering

Spin-dependent electron scattering could explain the GMR effect in the CIP geometry, regardless of whether it is mainly due to bulk or interface scattering. However, for a better understanding and tailoring of materials this question is certainly

interesting. On the other hand for two reasons a clear-cut distinction is not possible. First due to the uncertainty principle an electron has to be considered as more or less "extended" and therefore a localization strictly at an interface has no meaning. Second only bulk scattering within the mean free path away from the interface would contribute which further obscures the distinction between bulk and interface scattering. An excellent discussion of the situation has been given in a review by Levy, including the aspect of non-locality [60].

To get a clearer idea where the relevant scattering takes place Parkin [61] studied the dependence of the GMR effect on the thickness and position of Co and NiFe layers in layered structures of these materials with interlayers of Cu. He found that the scattering responsible for the effect is essentially located right at the interface. Reiss *et al.* [62] came to the same conclusion by measuring the GMR effect in a Fe/Cr multilayer during the growth of an Fe film. For the same system Schad *et al.* [63] could identify for epitaxial samples interface roughness as the main source of spin-dependent scattering, because the GMR effect increased both with the step height and the lateral step density at the Fe/Cr interface. On the other hand the dependence of GMR during the growth of NiFe in a NiFe/Cu structure yielded a NiFe thickness of 2.1 nm for the layer which contributes to the effect indicating that in this case both bulk and interface scattering are relevant [64].

3.4. Electron reflection at outer surfaces

Based on the mechanism shown in Fig. 7 a double layer should be as good as a multilayer if the outer surfaces are ideal mirrors for electrons. In the multilayers the largest effect so far observed at room temperature is 65% in a Co/Cu multilayer [65] whereas in double layers without special measures 9.9% is a respectable value [53]. An improvement of the electron reflectivity at the outer surfaces of a double layer therefore seems to be promising for an increase of the GMR effect. Analysis of experimental results from Fe/Cr layered structures [52] yielded specularity factors $p \approx 0.2$ where ideal reflection corresponds to $p = 1$.

Increase of the GMR effect in double layers due to an increase of the specularity was indeed found in the case of carefully prepared Co/Cu spin valves [57]. Structures prepared on NiO under oxygen partial pressures of 5×10^{-9} yielded record values around 17% at room temperature. Interesting enough 2 ML of Ta deposited on the surface were able to reduce the effect appreciably which was interpreted to be due to the roughness and decrease of the specularity introduced by the Ta.

4. TUNNEL MAGNETORESISTANCE (TMR)

An effect which is very similar to GMR using the CPP geometry is TMR. It is observed when the interlayer is insulating and tunnelling of electrons

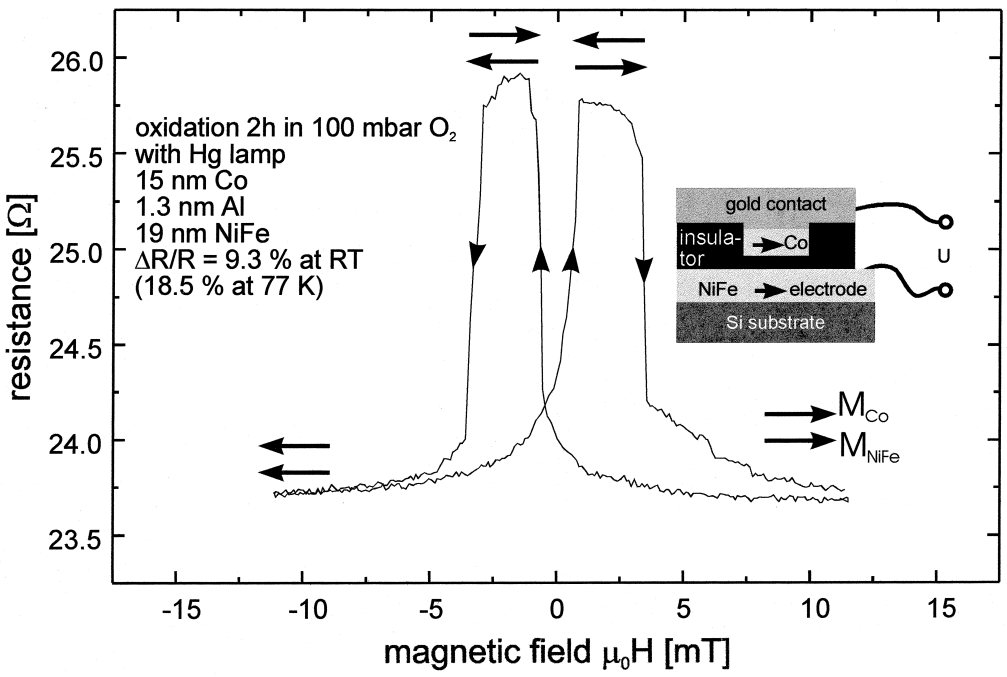

Fig. 8. TMR effect in a Co/Al/NiFe sample. A cross section of the structure is shown in the inset.

between the metallic ferromagnetic films across the interlayer occurs [12, 16, 17]. This is a truly quantum mechanical effect because without the associated overlap of the electron states of the metallic films it would not occur. Mostly Al_2O_3 is used as the insulating barrier. Typical relative tunnelling resistance changes which have so far been observed at room temperature are on the order of 20% with record values around 50% [66, 67]. Some data are in fair agreement with expectations based on the estimated degree of spin polarization of the conduction electrons at the metal/insulator interfaces. In other cases where the agreement is not as good it is not clear whether there is a problem with the sample preparation (e.g. remaining unoxidized Al) or whether the theory has to be modified.

An example for TMR is displayed in Fig. 8 [68, 69] where a cross section of the sample is shown in the inset. Antialignment is achieved for a certain external field range by using a hard (Co)/soft (NiFe) layer combination. The tunnelling barrier of Al_2O_3 is formed by oxidation of an Al layer under simultaneous exposure to UV light. A sheet resistance around 1 kΩ $(\mu m)^2$ was obtained here which is a moderate value compared to the value of 1 MΩ $(\mu m)^2$ when the Al_2O_3 is prepared by plasma oxidation. The latter value poses a problem with large RC times in the intended MRAM application. In Fig. 8 the size of the TMR effect is "only" 9.3% at RT but in the same structure 22.5% has been achieved [68, 69].

5. APPLICATIONS

Both "scientific" as well as "technical" applications of the effects described here have been reported. As a scientific application, the interlayer coupling can be used for example to monitor the electronic structure of materials—here used as interlayers—upon uptake of hydrogen [70, 71]. The GMR effect has been used to monitor the displacement and the speed of a domain wall in a nano wire [72].

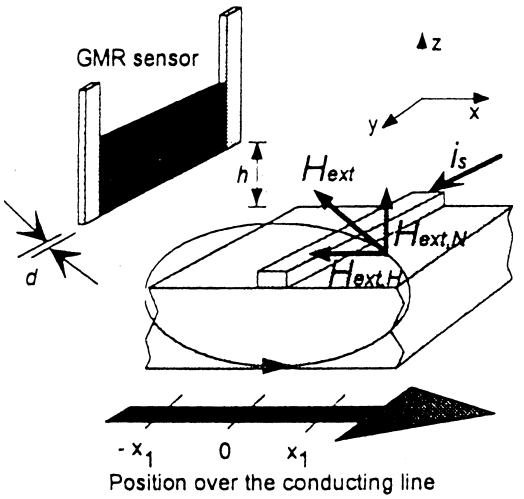

Fig. 9. Schematic arrangement for the measurement of the current distribution in a lead, suitable for testing integrated circuits.

The GMR effect can "technically" be applied in sensors for magnetic fields. One such case is for read out in hard disk drives (HDD) in computers [73]. The advantage of GMR over AMR is not only the larger signal but also that GMR is mainly an interface effect. This allows the sensor to be made thinner. As a result there is more flux concentration which further increases the sensitivity. Sensors for the HDD application are so small that despite the thin film structure the demagnetization effects due to finite lateral size already play an important role.

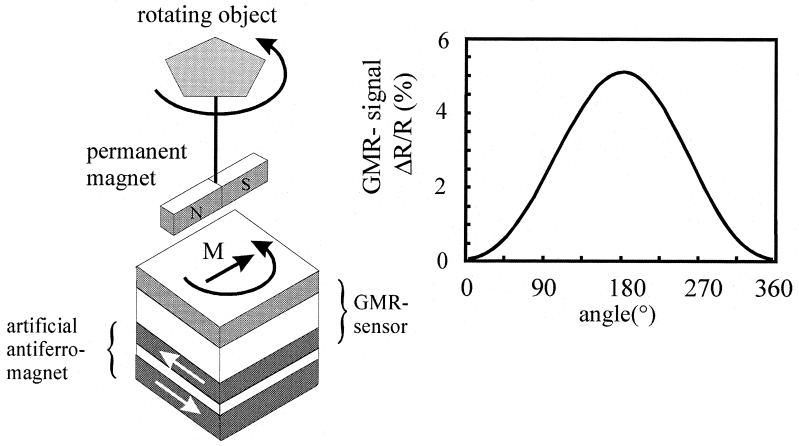

Fig. 10. Layered magnetic structure, including an "artificial antiferromagnet" (AAF, white arrows), for monitoring the angle of rotation of an object via the GMR effect. The GMR effect occurs between the detection layer (black arrow) and the upper film of the AAF. The response of the sensor to the rotation of the permanent magnet is shown on the right-hand side.

Hence the smaller thickness of a GMR-type sensor as compared to the AMR type allows the lateral size to decrease which makes it easier to hold the sensor on the track. The spatial resolution in read out can also be improved. This is the main reason why major hard disk manufacturers currently replace AMR by GMR.

From the foregoing it is clear that major advantages of GMR-type sensors are to be expected whenever miniaturization is an important aspect, like in a HDD. Figure 9 displays a further example. Here the GMR is used to test an integrated circuit (IC) in operation [74]. It takes advantage of the fact that currents produce magnetic fields. Due to the clear trend to make ICs ever smaller, a GMR-type sensor appears to be the best option for such a testing device. Further similar interesting applications can be expected in the wide field of microsystems technology.

Apart from the higher sensitivity, GMR sensors, as compared to those based on AMR, have the advantage of the full angular dependence. Whereas for an AMR-type sensor opposite field directions produce the same signal, for a GMR-type sensor parallel and antiparallel magnetization alignments are connected with different resistivities. The arrangement for the measurement of rotational angle is displayed in Fig. 10 (adopted from Ref. [75]). It includes also an application of the antiferromagnetic coupling, by using an "artificial antiferromagnet", consisting of three ferromagnetic films with strong antiferromagnetic coupling, such that the total moment cancels. Then the torque exerted by an external field vanishes and the field rotates only the magnetization in the detection layers. This rotation is monitored via the GMR effect and the measured signal is shown on the right-hand side.

Currently the TMR effect is mainly explored in view of the possibility of an application in future magnetic random access memories (MRAMs). The basic structure of one memory cell is indicated in the inset of Fig. 8. Parallel or antiparallel magnetization alignment would represent the two bit values 0 or 1. The GMR effect could basically also be considered for this application but the TMR effect clearly has the advantage of the inherently higher resistance of an element. In an MRAM this is important because of the large resistance of the current leads connecting a memory element with the processing unit. On the other hand the resistance should also not be too high because of the associated large RC times.

6. CONCLUSIONS

Research on layered magnetic structures clearly depends on the skill to prepare and structure such materials. In the case of research on interlayer coupling extremely good crystalline growth has been demonstrated for growth on Fe whiskers [30]. Unfortunately due to shunting by the whisker these samples are not suitable for GMR measurements. It remains a challenge to achieve similar quality on large semi-insulating substrates like Si or GaAs wafers. Improvements of MBE-type growth for example are possible with the use of surfactants [76]. If very good crystalline growth can be maintained in the case of interlayers consisting of layered structures, new phenomena can appear due to selective reflection and transmission of electrons [77, 78]. Concerning transport phenomena the maximum possible size of GMR and TMR is still an open issue. GMR has found an important application in sensors for hard disk drives. The question whether TMR will be used on a large scale in future MRAMs is still open.

Acknowledgements—I thank D. Buergler, P. Dederichs, and M. Stiles for fruitful discussions and proof-reading of the manuscript.

REFERENCES

1. Faraday, M., *Phil. Trans*., 1846, **136**, 1.
2. Kundt, A., *Wied. Ann*., 1884, **23**, 228.
3. König, H., *Optik*, 1948, **3**, 101.
4. Bean, C. P., in *Structure and Properties of Thin Films*, ed. C. Neugebauer, *et al*. Wiley, New York, 1959, p. 331.
5. Neel, L., *J. Phys. Radium*, 1954, **15**, 225.
6. Gradmann, U. and Müller, J., *Physica status solidi*, 1968, **27**, 313.
7. Takanashi, K., Mitani, S., Himi, K. and Fujimori, H., *Appl. Phys. Lett*., 1998, **72**, 737.
8. Salamon, M. B., Sinha, S., Rhyne, J. J., Cunningham, J. E., Erwin, R. W., Borchers, J. and Flynn, C. P., *Phys. Rev. Lett*., 1986, **56**, 259.
9. Majkrzak, C. F., Cable, J. W., Kwo, J., Hong, M., McWhan, D. B., Yafet, Y., Waszczak, J. V. and Vettier, C., *Phys. Rev. Lett*., 1986, **56**, 2700.
10. Grünberg, P., Schreiber, R., Pang, Y., Brodsky, M. B. and Sowers, H., *Phys. Rev. Lett*., 1986, **57**, 2442.
11. Thomson, W., *Proc. R. Soc*., 1857, **8**, 546.
12. Julliere, M., *Phys. Lett*., 1975, **54A**, 225.
13. Baibich, M. N., Broto, J. M., Fert, A., Nguyen-Van-Dau, F., Petroff, F., Etienne, P., Creuzet, G., Friederich, A. and Chazelas, J., *Phys. Rev. Lett*., 1988, **61**, 2472.
14. Binasch, G., Grünberg, P., Saurenbach, F. and Zinn, W., *Phys. Rev*., 1989, **B39**, 4828.
15. Fert, A., Grünberg, P., Barthelemy, A., Petroff, F. and Zinn, W., *JMMM*, 1995, **140–144**, 1.
16. Miyazaki, T. and Tezuka, N., *JMMM*, 1995, **139**, L231.
17. Moodera, J. S., Kinder, L. R., Wong, T. M. and Meservey, R., *Phys. Rev. Lett*., 1995, **74**, 3273.
18. Slonczewski, J. C., *JMMM*, 1995, **150**, 13.
19. Krebs, J. J., Lubitz, P., Chaiken, A. and Prinz, G. A., *Phys. Rev. Lett*., 1989, **63**, 1645.
20. Unguris, J., Celotta, R. J. and Pierce, D. T., *Phys. Rev. Lett*., 1992, **69**, 1125.
21. Hillebrecht, F. U., Roth, Ch., Jungblut, R., Kisker, E. and Bringer, A., *Europhys. Lett*., 1992, **19**, 711.
22. Turtur, C. and Bayreuther, G., *Phys. Rev. Lett*., 1994, **72**, 1557.
23. Bödeker, P., Hucht, A., Borchers, J., Güthoff, F., Schreyer, A. and Zabel, H., *Phys. Rev. Lett*., 1998, **81**, 914.

24. For a recent review see Pierce, D. T., Unguris, J., Celotta, R. J. and Stiles, M. D., *J. Magn. Magn. Mat*., 1999, **200**, 290.
25. Roth, Ch., Kleeman, Th., Hillebrecht, F. U. and Kisker, E., *Phys. Rev*., 1995, **B52**, R15691.
26. Grünberg, P., Demokritov, S., Fuss, A., Schreiber, R., Wolf, J. A. and Purcell, S. T., *JMMM*, 1992, **104–107**, 1734.
27. Grünberg, P., Wolf, J. A. and Schäfer, R., *Physica B*, 1996, **221**, 357.
28. Yan, S. S., Schreiber, R., Voges, F., Osthöver, C. and Grünberg, P., *Phys. Rev. B, Rapid Communications*, 1999, **59**, 11641.
29. Parkin, S. S. P. and Mauri, D., *Phys. Rev*., 1991, **B44**, 7131.
30. Unguris, J., Celotta, R. J. and Pierce, D. T., *Phys. Rev. Lett*., 1997, **79**, 2734.
31. Edwards, D. M., Mathon, J., Muniz, R. B. and Phan, M. S., *Phys. Rev. Lett*., 1991, **67**, 493.
32. Bruno, P., *Phys. Rev*., 1995, **B52**, 411.
33. Stiles, M. D., *J. appl. Phys*., 1996, **79**, 5805.
34. Johnson, M., *et al*., *Phys. Rev. Lett*., 1992, **68**, 2688.
35. Johnson, M., *et al*., *Phys. Rev. Lett*., 1992, **69**, 969.
36. Bloemen, P. J. H., *et al*., *Phys. Rev. Lett*., 1994, **72**, 764.
37. Okuno, S. N. and Inomata, K., *Phys. Rev. Lett*., 1994, **72**, 1553.
38. de Vries, *et al*., *Phys. Rev. Lett*., 1995, **75**, 4306.
39. Okuno, S. N. and Inomata, K., *J. Phys. Soc. Japan*, 1995, **64**, 3631.
40. Parkin, S. S. P., *Phys. Rev. Lett*., 1991, **67**, 3598.
41. Mathon, J., Villeret, M., Edwards, D. M. and Muniz, R. B., *JMMM*, 1993, **121**, 242.
42. Zoll, S., *et al*., *Europhys. Lett*., 1997, **39**, 323.
43. Fullerton, E. E., Stoeffler, D., Ounadjella, K., Heinrich, B., Celinski, Z. and Bland, J. A. C., *Phys. Rev*., 1995, **B51**, 6364.
44. Hicken, R. J., *et al*., *Phys. Rev*., 1994, **B50**, 6143.
45. Yan, S., *et al*., *Phys. Rev*., 1995, **B52**, 1107.
46. Vohl, M., Barnas, J. and Grünberg, P., *Phys Rev B*, 1989, **39**, 12003.
47. Mirbt, S., Niklasson, A. M. N., Johansson, B. and Skriver, H. L., *Phys. Rev*., 1996, **B54**, 6382.
48. Fullerton, E. E., Mattson, J. E., Lee, S. R., Sowers, C. H., Huang, Y. Y., Felcher, G. and Bader, S. D., *J. appl. Phys*., 1993, **73**, 6335.
49. Briner, B. and Landoldt, M., *Phys. Rev. Lett*., 1994, **73**, 340.
50. Chaiken, A., Michel, R. P. and Wall, M. A., *Phys. Rev*., 1996, **B53**, 5518.
51. de Vries, J. J., *et al*., *Phys. Rev. Lett*., 1997, **78**, 3023.
52. Barnas, J., Fuss, A., Camley, R. E., Grünberg, P. and Zinn, W., *Phys. Rev*., 1990, **B42**, 8110.
53. Shinjo, T. and Yamamoto, H., *J. Phys. Soc. Japan*, 1990, **59**, 3061.
54. Pratt, W. P., *et al*., *Phys. Rev. Lett*., 1991, **66**, 3060.
55. Gijs, M. A. M., *et al*., *Phys. Rev. Lett*., 1993, **70**, 3343.
56. Mott, N., *Proc. R. Soc*., 1963, **156**, 368.
57. Egelhoff, W. F., *et al*., *J. appl. Phys*., 1997, **82**, 6142.
58. Butler, W. H., *et al*., *Phys. Rev. Lett*., 1996, **17**, 3216.
59. Zahn, P., *et al*., *Phys. Rev. Lett*., 1998, **80**, 4309.
60. Levy, P. M., *Solid St. Phys*., 1994, **47**, 367.
61. Parkin, S. S. P., *Phys. Rev. Lett*., 1993, **71**, 1641.
62. Reiss, G., *et al*., *JMMM*, 1998, **184**, 281.
63. Schad, R., *et al*., *Phys. Rev*., 1999, **B59**, 1242.
64. Hütten *et al*., *Acta mater*., 1999, **47**, 4245.
65. Parkin, S. S. P., Li, Z. G. and Smith, D. J., *Appl. Phys. Lett*., 1991, **58**, 2710.
66. Gallagher, W. J., *et al*., *J. appl. Phys*., 1997, **81**, 3741.
67. Parkin, S. S. P., Private communication.
68. Rottländer, P. *et al*., submitted.
69. Girgis, M. *et al*., submitted.
70. Klose, F., Rehm, Ch., Nagengast, D., Maletta, H. and Weidinger, A., *Phys. Rev. Lett*., 1997, **78**, 1150.
71. Hjörvarsson, B., Dura, J. A., Isberg, P., Watanabe, T., Udovic, T. J., Andersson, G. and Majkrzak, C. F., *Phys. Rev. Lett*., 1997, **79**, 901.
72. Shinjo, T., Private communication.
73. http://www.research.ibm.com/research/gmr.html.
74. Bae, S., Schlensog, A., Mertin, W., Kubalek, E. and Maywald, M., *Microelectronics Reliability*, 1998, **38**, 969.
75. http://www.infineon.com/products/38/pdf/gmr.pdf.
76. Camarero, J., Graf, T., de Miguel, J. J., Miranda, R., Kuch, W., Zharnikov, M., Dittschar, A., Schneider, C. M. and Kirschner, J., *Phys. Rev. Lett*., 1996, **76**, 4428.
77. Okuno, S., Private communication.
78. Bürgler, D. *et al*., *Phys. Rev*., 1999, **B60**, R3732.